ELSEVIER

The effect of changes in relative humidity on the hydration rate of Pachuca obsidian

Lawrence M. Anovitz [a,b,*], Lee R. Riciputi [c], David R. Cole [b],
Miroslaw S. Gruszkiewicz [b], J. Michael Elam [d]

[a] *Department of Earth and Planetary Sciences, University of Tennessee, Knoxville, Tennessee 37996, United States*
[b] *Chemical Sciences Division, MS 6110, P.O. Box 2008, Bldg. 4500S, Oak Ridge National Laboratory, Oak Ridge, Tennessee 37831-6110, United States*
[c] *Chemical Sciences Division, MS 6375, P.O. Box 2008, Bldg. 4500S, Oak Ridge National Laboratory, Oak Ridge, Tennessee 37831-6375, United States*
[d] *Department of Anthropology, University of Tennessee, Knoxville, Tennessee 37996, United States*

Abstract

The effect of relative humidity on the hydration rate of obsidian and other glasses has been debated since the early work of [I. Friedman, R. Smith, Am. Antiquity 25 (1960) 476]. While more recent work has been in general agreement that a relative humidity dependence does exist, hydration profiles as a function of relative humidity have not been obtained. In this paper we present the results of a study in which samples of Pachuca obsidian were hydrated for approximately 5 days at 150 °C at relative humidities ranging from 21% to 100%, and the resultant profiles were measured by secondary ion mass spectrometry (SIMS). The results suggest that the hydration rate is, indeed, a function of relative humidity, but for the relative humidity levels commonly observed in most soils the effects on hydration dating are expected to be relatively small. In addition, analysis of the surface values as sorption isotherms and comparisons with nitrogen sorption isotherms suggests that water is relatively strongly bound to the obsidian surface. By assuming a situation in which the 'surface' refers to active centers within the glass we have shown that an adsorption model provides a useful approach to modeling the diffusive process.
© 2006 Elsevier B.V. All rights reserved.

1. Introduction

Since the initial suggestion by Friedman and Smith [1] that the extent of hydration of an obsidian artifact could be used to date that artifact, there has been significant discussion as to the extent to which environmental variables such as temperature, burial history, and relative humidity affect the hydration rate [2–9]. While temperature was recognized early on as an important variable, the importance of relative humidity has been less certain, and the discussion more lengthy.

As summarized by Friedman et al. [9], in their initial work Friedman and Smith [1] assumed that obsidian hydration was not a function of relative humidity, because obsidians in dry and wet environments appeared to hydrate at the same rate. Friedman and Long [3] appeared to confirm this assumption with experiments conducted from 1 to 136 atmospheres, 95 °C to 245 °C, but Friedman et al. [9] noted

---
* Corresponding author. Address: Chemical Sciences Division, MS 6110, P.O. Box 2008, Bldg. 4500S, Oak Ridge National Laboratory, Oak Ridge, Tennessee 37831-6110, United States. Tel.: +1 865 574 5034; fax: +1 865 574 4961.
   E-mail address: anovitzlm@ornl.gov (L.M. Anovitz).

that additional, lower temperature experiments suggested that the hydration rate did indeed depend on relative humidity. Later work [7–9] confirmed this dependence. Additional experiments on the effects of relative humidity on synthetic glass hydration rates have been reported by several authors [8,10–16].

This question has been further complicated by the work of Anovitz et al. [17] who noted, in part, that the optical techniques commonly used for analysis of obsidian hydration are highly imprecise. In two of the studies mentioned above, however, optical techniques were used to examine the experimental samples [3,7]. Thus, the measurements made in these studies are of uncertain precision and accuracy.

This paper presents the results of a study evaluating the effects of reduced relative humidity on obsidian hydration rates using high-precision secondary ion mass spectrometry (SIMS) analyses to quantify the diffusion profiles, and considers the factors leading to the observed effects.

2. Experimental method

The experimental and analytical techniques used in this study have been described elsewhere [17–20]. Thus, except for the method used for relative humidity control, they will only be described briefly here.

The experiments reported here were performed using obsidian from the Pachuca source, located in the Sierra Madre Oriental northeast of the Basin of Mexico. The outcrops cover a large area near the town of Huasca, Hidalgo. Pachuca obsidian is green, and shows a schiller in some directions due to microscopic vessicles. The materials used for our experiments are largely free of inclusions, although a few exist that were avoided during sample selection. Experimental samples were manufactured by polishing both sides of plates cut from obsidian blocks, then cutting those plates into smaller blocks approximately 2–3 mm on a side.

Experiments were conducted in reaction vessels fabricated from VCR®-type vacuum fittings. To prepare the vessels, seals were polished and the vessels subsequently washed with water, acetone and ethanol, and baked dry at 150 °C. All experiments described herein were carried out at 150 °C, and initiated simultaneously. To do so, vessels were placed in a covered aluminum block containing wells for ten vessels in a convection oven. Temperatures were monitored by three resistance temperature detectors (RTD's) inserted in tight-fitting wells in this block. Additional thermal mass for temperature stability was obtained by setting the aluminum block on a 2 inch thick steel plate.

In earlier experiments it was determined that the initial heating time was relatively long if all ten vessels at room temperature were placed simultaneously into an Al-block pre-heated to the experimental temperature. In order to increase the heating rate, the vessels were first placed in boiling water (at $t = 0$ min) prior to insertion into the furnace, and the Al block was preheated to 175 °C. The vessels were then removed from the water and inserted in the furnace in order between $t = 11$ and $t = 20$ min, during which time the temperature of the Al block began to decrease due, in large part, to the thermal mass of the cooler vessels. The lid was replaced on the Al block and the furnace closed at $t = 20$ min. At $t = 25$ min the block reached a minimum temperature of 138 °C. This was assumed to be the point where the temperature of the vessels reached that of the surrounding portions of the Al block, and the temperature of the oven was then slowly lowered back to 150 °C. The beginning of the experiment was somewhat arbitrarily defined as the time at which the block/vessel assembly reached 148 °C, 80 min after the vessels were placed in the boiling water. After the initial heating period temperatures recorded over the lifetime of the experiment varied by less than 0.5 °C. The experiment was terminated by removing the vessels from the block and quenching them in cold water. The total duration of the experiment was 5 days, 17 h, and 18 min.

Prior to assembly, sufficient water was placed in a Teflon cup seated in the vessel bottom to produce a saturated two-phase liquid-vapor system at the temperature of interest. Samples to be hydrated were placed on a steel mesh support suspended in the vapor phase. Under these conditions the chemical potential of water at the surface of the glass remains identical to its value in the liquid, but the solubility of the glass in the vapor is several orders of magnitude less than in the liquid [21,22]. Thus, this experimental design allows diffusion to be studied independently from dissolution.

After each vessel was quenched it was then opened and the samples were placed in small plastic 'freezer bottles' sealed with an o-ring and transferred as quickly as possible to a freezer at ~ -25 °C. All samples were stored in this freezer from the time of the experiment until the time of analysis in order to limit any changes during storage.

In order to control the relative humidity (rH, the ratio of the actual vapor pressure of water to that in the pure H_2O system at the same temperature) to which the samples were exposed, an aliquot of distilled, deionized water, obtained from a Barnstead NANOpure ion exchange ultrapure water system, with a conductivity of approximately 18.3 MΩ, was mixed with various concentrations of LiBr. The concentration of LiBr in the solution was varied in order to reduce the activity of water in the solution, and thus the fugacity (or partial pressure) of water in the vapor phase. Fig. 1 shows the activity of water as a function of the concentration of this and other salts at 150 °C (MgCl₂ [23]; CaCl₂ [24]; NaCl [25,26]; LiCl [27–29]; LiBr [29]). The low volatility of salts assured that little LiBr would contact the obsidian surface via vapor phase transport [22,30]. LiBr was chosen because high-precision measurements of the vapor pressure of LiBr/H_2O solutions had just been completed by one of us (MSG), and because the range of concentrations, while not extending to saturation, was sufficient for the planned experiments. The concentrations
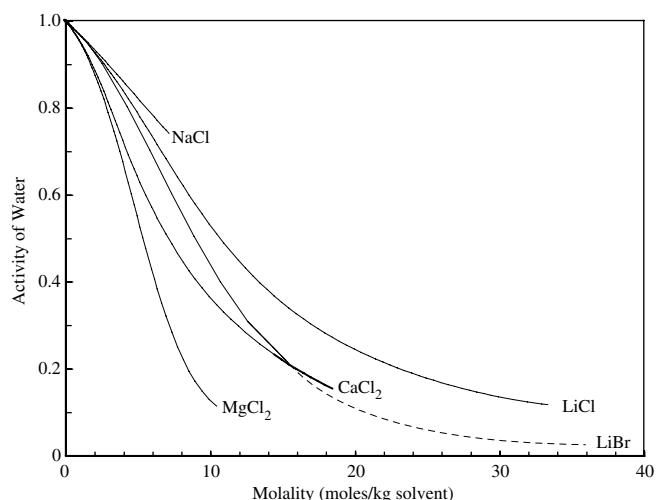
Fig. 1. Activity of water as a function of the concentration of several salts at 150 °C: MgCl$_2$: Wang et al. (1998); CaCl$_2$: Gruszkiewicz and Simonson (2005); NaCl: Pitzer et al. (1984); Archer (1992); LiCl: Gibbard and Scatchard (1973); Holmes and Mesmer (1983); Gruszkiewicz, unpb., and LiBr: Gruszkiewicz, unpb. Data for LiBr have only been measured up to 15.4631 molal. The dashed line extrapolated to higher molalities is only meant to show that saturation has not been reached with the available data, and not as an estimate of values at higher molalities.

Table 1
Concentrations of LiBr and associated relative humidities

Vessel	Molality LiBr (moles/kg solvent)	Percent relative humidity
1	0	100
2	1.4893	95.041
3	2.5800	90.010
4	4.3210	80.074
5	5.8750	70.108
6	7.3990	60.084
7	8.9482	50.246
8	10.762	39.811
9	12.652	30.717
10	15.463	21.167

Data from Gruszkiewicz (unpublished).

used, and the associated relative humidities, are listed in Table 1. A similar approach was used by [9], who placed their experimental powders over saturated potassium chloride and magnesium chloride solutions, although they did not take advantage of the possibility of using undersaturated solutions to achieve a broader range of *rH* values.

SIMS analysis was used to examine the hydrogen concentration gradients formed during hydration. For most of these depth-profile analyses, the primary beam consisted of mass-selected, negatively-charged, ^{16}O primary ions accelerated at 12.5 keV. The beam had a diameter of ~50 μm and a current of ~130 nA, and was rastered over an area of 150 × 150 μm to produce a well-shaped (roughly square) crater with a flat bottom. Only ions from the central 33 μm of this crater were transmitted through the secondary mass spectrometer for analysis. Crater depths were measured using a Tencor Alpha-Step 200 profilometer that provided a depth uncertainty of 0.05 μm.

3. Results and discussion

Fig. 2 shows the SIMS analyses for the experiments described in Table 1. Descriptive details and analyses of these profiles are provided in Table 2. Several features are readily apparent. First, as we have noted previously [17–20] and as was reported before us by others [31–40], the curves are s-shaped implying that the diffusion coefficient is concentration-dependent. The data shown in Fig. 2, however, also suggest that the shape is not affected, at least qualitatively, by the external relative humidity, as each of the curves has essentially the same shape.

Secondly, it is apparent from Fig. 2 that the maximum hydrogen concentration increases as a function of *rH*. While the measured maxima are slightly removed from the surface, as we have discussed previously [17–20] this appears to be an analytical artifact, and the measured maximum is taken to be a projection of the actual surface concentration. The measured maxima are shown as a function of relative humidity in Fig. 3.

The dependence of the maximum or surface concentration on relative humidity is somewhat unexpected. Comparison of experimental and archaeological data over a range of temperatures [18–20] does not suggest a major change in the maximum hydrogen content of the glass with temperature although a change with time is indicated. As those experiments were all done at pressures along the liquid/vapor curve, which vary from 4.7572 bars at 150 °C to 0.023388 bars at 20 °C [41], no significant change with $p(H_2O)$ (or *rH*) was expected in the experiments presented here.

If, in fact, the solubility of water in the glass is structurally controlled, perhaps somewhere near complete Q(3) saturation of the silicon-oxygen bonds (one H per silicon), then it is reasonable for the saturation value to be essentially independent of temperature and pressure. The *rH* dependence observed in the isothermal, reduced relative
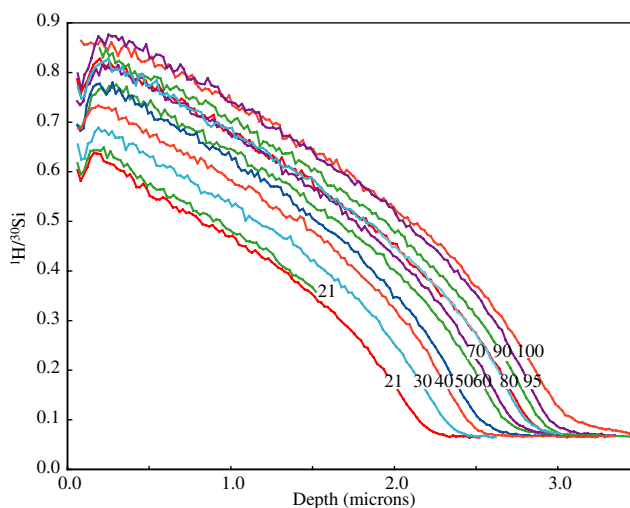

Fig. 2. SIMS depth-profile analyses for the experiments outlined in Table 1.

Table 2
Fitted and calculated parameters for each profile

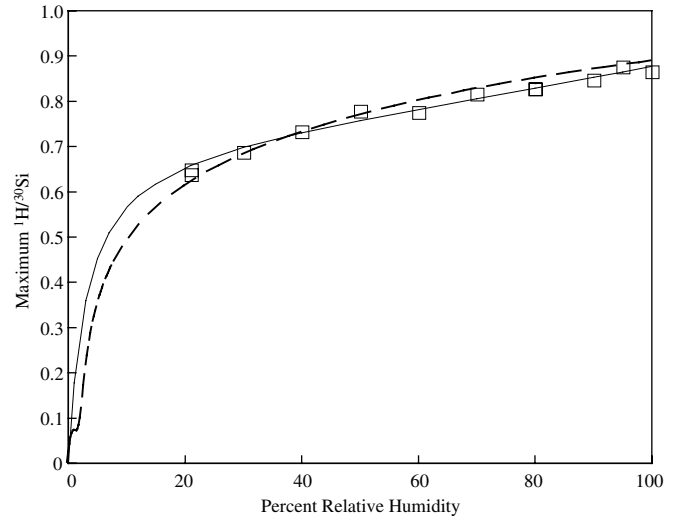| Percent relative humidity	Maximum ^{1}H/^{30}Si	Half-fall distance (μm)	Half-fall ^{1}H/^{30}Si	Relative time (seconds)	Percent relative time	D_{ch} (Eq. 1) (μm²/s)	D_{ch} (Eq. 2) (μm²/s)	Modified BET calculated maximum ^{1}H/^{30}Si	Integral (background subtracted)	Langmuir integral fit
100	0.866	2.42	0.46675	494280	100	1.18E-05	1.30E-05	0.877	1.640	1.505
95	0.876	2.36	0.47175	470074	95.1	1.13E-05	1.24E-05	0.865	1.613	1.487
90	0.847	2.26	0.45725	431081	87.2	1.03E-05	1.14E-05	0.853	1.494	1.468
80	0.828	2.21	0.44775	412218	83.4	9.88E-06	1.09E-05	0.829	1.414	1.423
80	0.828	2.23	0.44775	419713	84.9	1.01E-05	1.11E-05	0.829	1.416	1.423
70	0.816	2.16	0.44175	393777	79.7	9.44E-06	1.04E-05	0.806	1.369	1.370
60	0.776	2.12	0.42175	379327	76.7	9.09E-06	9.99E-06	0.782	1.278	1.305
50	0.779	1.97	0.42325	327548	66.3	7.85E-06	8.63E-06	0.757	1.193	1.224
40	0.733	1.97	0.40025	327548	66.3	7.85E-06	8.63E-06	0.730	1.092	1.119
30	0.688	1.78	0.37775	267413	54.1	6.41E-06	7.05E-06	0.698	0.955	0.980
21	0.649		0.35825					0.659		0.807
21	0.638	1.70	0.35275	243916	49.3	5.85E-06	6.43E-06	0.659	0.794	0.807

Experimental time: 5 days, 17 h, 18 min.

Fig. 3. Maximum analyzed ^{1}H/^{30}Si values from the depth-profiled experiments as a function of relative humidity. The solid curve shown is a modified BET fit to the data, and the dashed curve shows the results of the diffusion with adsorption model.

humidity experiments thus suggests one of two alternative explanations: either (1) reducing relative humidity slows the rate of surface sorption, and the observed changes parallel those observed at 100 percent relative humidity as a function of time, or (2) the surface saturation value is, in fact, controlled by a thermodynamic equilibrium with the surrounding vapor. If the latter is true, the observed temperature independence may reflect changes in the activity of water in the glass relative to the saturation concentration or offsetting vapor density and thermal effects, and not the water fugacity at a given temperature. The slow rate at which surface equilibrium is obtained makes experimental (or even archaeological) determination of the surface equilibrium value difficult, however, and currently available data are insufficient to quantify this issue.

Doremus [42] noted that the ratio of the concentration of a gas molecularly dissolved (unreacted) in the glass to its fugacity in the gas phase, known as the Ostwald solubility, is constant over wide ranges of pressure and temperature in a variety of silicate glasses. This is essentially a restatement of Henry's Law, and is generally confirmed in our study by the linear dependence of the maximum hydrogen content on the relative humidity down to 20% rH, and the apparent temperature independence at 100% rH just discussed. Doremus [42] concluded that this implies very little interaction of the dissolved molecules with the surrounding glass network. This would appear consistent with the low concentration of hydroxyl groups high-temperature models predict for the conditions of these experiments e.g. [43].

It is also apparent from Fig. 2 that increases in relative humidity significantly increase the depth of the hydration profile. We can quantify this by characterizing each profile with a half-fall depth. As we have noted in our previous work [18,20], the depth of the diffusion profile can be

conveniently represented in terms of one of several 'characteristic depths' that characterize the profile as a single point. This point can be any value, such as the half-fall distance or the distance to the inflection point, that is readily identifiable for any profile of interest, and can be converted into a characteristic diffusion coefficient as:

$$x_{HF}^2 = D_{CH}t. \tag{1}$$

Half-fall depths and characteristic diffusion coefficients for the profiles shown in Fig. 2 are listed in Table 2, and the latter are shown in Fig. 4. As can be seen, both appear to decrease with decreasing relative humidity. While we have already shown experimentally [44] that diffusion depth in Pachuca obsidian does not go as the square-root-of-time, this will not be a factor in this analysis, as all samples were run for the same length of time.

Implicit in Eq. (1) is the assumption that the surface concentration, C_0, is a constant. As we know from Fig. 2, however, this is not correct, but the effect of this difference remains uncertain. Eq. (1) is related to the equation for diffusion into a semi-infinite medium from a constant surface concentration [45]:

$$\left(\frac{C - C_1}{C_0 - C_1} \right) = erfc\left(\frac{x}{2\sqrt{D_{CH}t}} \right), \tag{2}$$

where x is the depth of the characteristic point, C the concentration at that point, t the time, C_1 the background concentration and C_0 the surface concentration. If Eq. (1) is plugged into the right-hand-side of Eq. (2), then the value of the left hand side is approximately 0.5, and thus x defined by Eq. (1) is approximately the half-fall distance. There is a slight difference between the D_{ch} values calculated from Eqs. (1) and (2) for a left-hand-side value exactly 0.5, and both values are given in Table 2 and shown in Fig. 4. However, as can be seen from Eq. (2), changing C_0 has no effect on the half-fall distance.
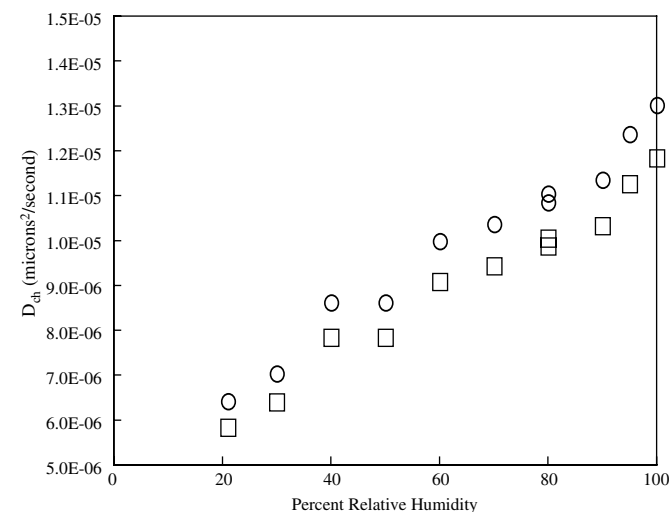
Two factors suggest, however, that this analysis is insufficient. First, as shown by the shape of the diffusion profile, the diffusion coefficient is concentration-dependent, and increases with increasing hydrogen content. Thus, a lower surface concentration would imply a lower diffusion coefficient, and thus a smaller half-fall distance, as observed in our experiments. Second, as discussed above, available data [18,19] suggest that surface concentration increases with time, again influencing the overall evolution of the diffusion profile. Thus, the apparent decrease in the characteristic diffusion coefficient with decreasing relative humidity may be an artifact of the mathematical analysis.

3.1. Sorption analysis

If it is true that the maximum concentrations, as proxies for the surface concentrations, represent equilibrium between the relative humidity in the vapor phase and the concentration in the glass, then Fig. 3 can be treated as an adsorption isotherm and modeled accordingly. It is well known that hydrophilic glassy polymers tend to fit a standard Brunauer-Emmett-Teller (BET) isotherm only at relatively low relative humidities because the model assumes that infinite sorption will occur at 100% rH [46–50]. Brunauer et al., [49], see also, [51] therefore modified the BET model to account for finite sorption at saturated conditions. This modification allowed the equation to fit an upturn in the otherwise linear BET equation at high values of p/p_0 observed in many systems, and was theoretically justified by noting that 'although it is true that at p_0 an infinite number of *liquid* layers can build up on the adsorbent, …an infinite number of *adsorbed* layers does not…BET assumed that liquid and adsorbed layers are indistinguishable at this point, but this is not necessarily true…'

Writing the modified BET equation in linear form in terms of the variables adopted here yields:

$$\frac{rH}{C_0(1 - k * rH)} = \frac{1}{C_{0,m}\psi k} + \left(\frac{\psi - 1}{C_{0,m}\psi} \right)rH, \tag{3}$$

where rH is the relative humidity (given as a fraction of 1), ψ is the BET parameter, C_0 is the surface (or maximum) concentration at a given relative humidity, $C_{0,m}$ is the monolayer sorption, and k is a fitting parameter related to the limit on the number of surface sorbed layers that permits $C_0/C_{0,m}$ to tend to infinity at a hypothetical relative humidity greater than 1. This equation is, in fact, identical to the Guggenheim-Anderson-De Boer (GAB) model widely used to describe water sorption in foods and natural polymers [50–53]. As can be seen in Fig. 3, this equation fits our data very well, with the coefficients $\psi = 163.99$, $k = 0.2$, and $C_{0,m} = 0.71877$, yielding an r^2 value of 0.9992 and a 1σ value of 0.012. From this, we can calculate the approximate difference between the molar enthalpy of adsorption of water on the glass and the molar enthalpy of condensation of water as:

Fig. 4. Calculated characteristic diffusion coefficients as a function of relative humidity calculated from Eq. (1) (squares) and Eq. (2) (circles).

$$\psi = \exp\left(\frac{E_A - E_L}{RT}\right), \tag{4}$$

yielding $E_A - E_L = 17.943$ kJ/mol. The enthalpy of condensation for water (E_L) at 150 °C is 38.740 kJ/mol [54], and thus the enthalpy of adsorption of water on the glass is approximately 56.683 kJ/mol. Enthalpy of adsorption calculated in this manner is, however, typically somewhat smaller than that obtained calorimetrically [49]. In part, this may be because isosteric heats of adsorption obtained calorimetrically typically vary with the percent coverage of the surface, often decreasing towards the value for the condensation of water at high coverage.

The value obtained from our data is, nonetheless, within the range obtained for similar materials. For example, Takei et al. [55] obtained a ψ value near 400 for a porous silica glass from BET measurements at 0 °C, which corresponds to an E_A-E_L value of 13.6 kJ/mol, and Puibasset and Pellenq [56,57] obtained model E_A values for Vycor glass that begin at 78 kJ/mole for the initial hydration increments. Several studies of water adsorption on silica gel at temperatures just above room temperature [58–61] yield $E_A - E_L$ values from near zero to about 5.5 kJ/mol. Matsumoto et al. [62] showed that mesoporous silica FSM-16 was initially hydrophobic, with an E_A value of approximately 20 kJ/mole for initial adsorption, but that this changed to a hydrophyllic value of 70 kJ/mol during a second run on the same material. Isopiestic measurements by Gruszkiewicz et al. [63] on water adsorption on rock samples from the Geysers hydrothermal field yielded $E_A - E_L$ values between 3.5 and 8.5 kJ/mol.

The modified BET fit also predicts that, at saturation, the statistical number of adsorbed layers is only 1.22. This is consistent with the relatively flat slope of the sorption curve in Fig. 3, which suggests that little water is adsorbed by the sample beyond its monolayer capacity. In addition, the lower limit of the linear region of the isotherm lies at approximately $rH = 0.4$. The hydrogen-concentration profile for the experiment at $rH = 0.4$ had a near-surface maximum ^{1}H/^{30}Si value of 0.733, which is very close to the fitted value of $C_{0,m}$.

These results can be compared with those from a standard nitrogen adsorption isotherm for a powdered Pachuca obsidian sample (Fig. 5). This is a classic type II-b isotherm, implying that the material is nonporous, but that nitrogen condensed between the powder particles shifts to a lower-energy configuration at high pressure, leading to the observed hysteresis. Fitting these data to the standard BET equation in the range $0.05 < P/P_0 < 0.35$ yields $\psi = 34.75$, a monolayer capacity of $1.118 \cdot 10^{-3}$ g N$_2$/g sample, and a correlation coefficient of 0.9998. The relatively low value of ψ suggests that nitrogen/glass interactions are relatively weak, much weaker than that of water with the surface, with approximately 14.5% of the surface still uncovered when multilayer development begins, and an $E_A - E_L$ value of only 12.483 kJ/mol. Thus water appears to sorb more strongly to the obsidian than does nitrogen.
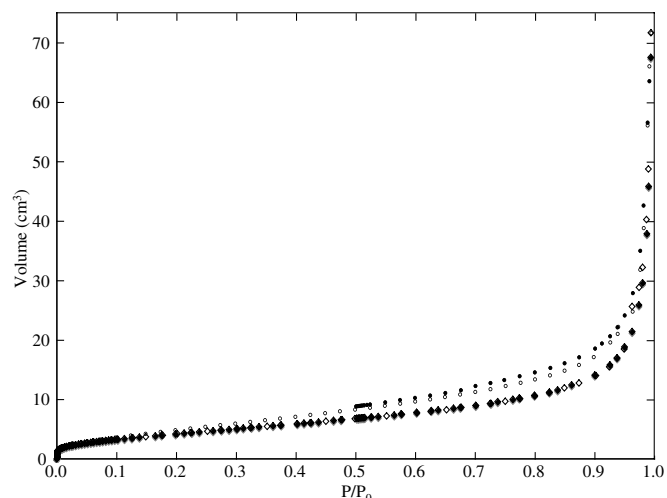

Fig. 5. A standard nitrogen adsorption (diamonds)/desorption (circles) isotherm for a powdered Pachuca obsidian sample. Two isotherms were measured on the same sample. One is shown as filled symbols, the other as open symbols.

One difficulty with modeling the surface hydrogen concentrations as an adsorption isotherm is that adsorption models typically do not consider that the adsorbate may diffuse into the adsorbent, which is clearly the case in our experiments. Fig. 6 shows the integrated hydrogen sorption over the whole diffusion profile as a function of relative humidity. Qualitatively, this curve is very similar to those for the surface maxima. However, except for the three highest relative humidity samples this curve can be fit to the much simpler Langmuir equation that, from the point of view of surface sorption, assumes only monolayer coverage:

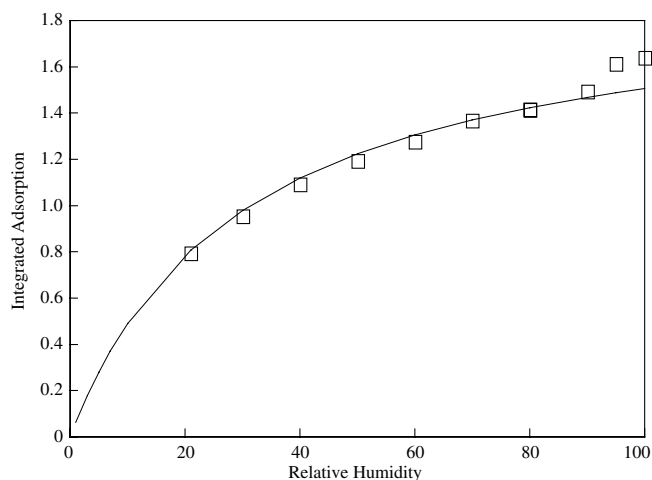$$\frac{n}{n_L} = \frac{b^* rH}{1 + (b^* rH)}, \tag{5}$$

Fig. 6. The integrated hydrogen content over each of the hydration profiles as a function of relative humidity. Background values have been subtracted from each total. The curve is a fit to the data using the Langmuir equation.

where n is the integrated hydrogen content and n_L and b are empirical constants. For surface sorption, n/n_L is the fraction of occupied surface monolayer sites. Fitting this equation to the integrated sorption data yields $n_L = 1.95451$ and $b = 3.35$. Doremus [42] used a similar approach to model both the water speciation and solubility of water in silicate glasses and melts noting that, as with surface monolayer sites, the number of reactive sites in the glass is limited, and saturates at high water contents. This may well explain the apparent fit of our integrated hydrogen-content data to the Langmuir equation.

Thus, both the surface maxima and the total integrated sorption data fit surface sorption profiles, suggesting that surface sorption processes are important controls on the overall rate of adsorption into the glass. In addition, surface relaxation may be an important process controlling the time-dependence of the near-surface maximum [19].

3.2. Comparison with previous work

As noted in the introduction, experiments on the effects of relative humidity on glass hydration rates have been carried out by several authors [3,7,9,10,12–16]. Qualitatively, all of these experiments, except those of Friedman and Long [3], agree with our result that hydration rate is a function of relative humidity. Unfortunately, the data on which Friedman and Long [3] based their initial conclusion that hydration rate was not effected by relative humidity were not presented in their paper but, as noted above, this conclusion was later modified.

There are, however, several quantitative differences. The most important is that several studies [7,9–11,13,15] suggest a much larger apparent decrease in the diffusion rate with decreasing relative humidity at relatively high rH values than do our results (Fig. 7). Our data suggest that D_{ch} (in $\mu m^2/s$) decreases approximately linearly with rH, but only by a factor of two from 100% rH to 20% rH. By comparison, data from some of these other experiments (modified as necessary to distance^2/time units) suggest a much more rapid decrease in D_{ch} with decreasing relative humidity.

In part, the differences between these datasets may be methodological, but glass composition may also have played an important role. For instance, the data of Mazer et al. [7] were measured optically, and our previous work has shown that this approach is subject to significant uncertainties. In addition, the data of Mazer et al. [7] suggest that temperature may also play an important role in the effect of relative humidity on diffusion. Bartholomew et al. [10] performed their measurements by heating hydrated synthetic silicate glasses in air to remove the hydrated layers, then measuring the difference between the initial and final sample thicknesses. While the hydration depths were large (> 1 mm), the accuracy of this technique is uncertain. The data of Friedman et al. [9] were obtained on obsidian powders. Despite careful drying, surface chemisorption on powders may dominate bulk diffusive
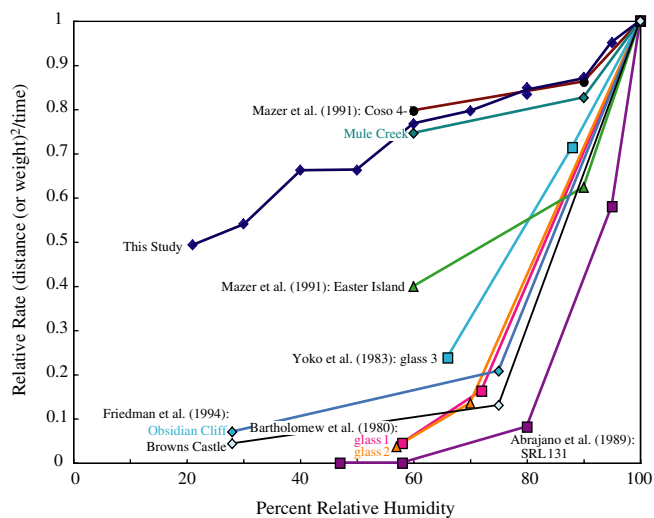

Fig. 7. Comparison of relative humidity effects observed in different experiments. All data have been modified if necessary to distance^2/time units, and the results of each study are normalized to the value at 100% relative humidity.

effects when total water uptake is measured. Abrajano et al. [15] measured hydration rates on nuclear waste glasses with relatively low-Si contents (44.0 wt.% in glass SRL 131). Experiments to test the effects of relative humidity were analyzed by measuring the altered layer of these glasses using either SEM or SIMS. Hydrogen profiles were not measured, but the mechanisms by which these glasses alter appear to differ significantly from those affecting obsidian.

It is somewhat more difficult to judge whether previous experimental data support our conclusions about changes in surface concentration (or near-surface maxima) with changes in relative humidity, as none directly measured hydrogen contents as a function of depth. Nonetheless, several did address changes in overall solubility with rH. Both Bartholomew et al. [10] and Tomozawa et al. [14] measured the water contents of their glasses by loss-on-ignition, and found that water content decreased with decreasing rH. Yoko et al. [13] found that the solubility of water in the hydrated layer of their glasses was dependent on both temperature and relative humidity, but their data are insufficient to separate these effects. Tomozawa et al. [14] found that the decrease in water content with decreasing rH was relatively small from saturation to $rH = 20\%$, decreasing only about 25%, in agreement with our data. This is a somewhat smaller change than that observed in a borosilicate glass by Tomozawa and Tomozawa [16] who found total solubility to be proportional to the square-root of water pressure. In all cases, however, the positive correlation between relative humidity and solubility appears clear.

The overall hydrogen-sorption isotherm calculated from our data (Fig. 6) combines the effects of diffusion rates and overall solubilities. As noted above, except for the highest rH values, our data closely approximate a Langmuir isotherm, and even at relatively high rH the increase in total

sorption is relatively small. This contrasts with the results of Mazer et al. [7], obtained by gravimetric analysis of crushed obsidian samples hydrated at 23 °C. These data look much like a type-II isotherm similar in shape to the adsorption branch of our nitrogen data (Fig. 5), with a 'knee' at approximately $rH = 3\%$. Following Hagymassy et al. [64] and Ebert et al. [8], Mazer et al. [7] interpreted their data as a sorption isotherm. They attributed the initial increase to formation of a statistical monolayer of hydrogen-bonded water on silanol groups, and the remainder of the profile first to additional silanol formation, then to formation of a surface film at high rH.

The study of Ebert et al. [8] is the only one to report desorption, as well as adsorption isotherms on powders (30–45 μm, 62 m²/g calculated surface area), and data are provided for both an obsidian from Coso Hot Springs, Inyo CA, and a borosilicate nuclear waste glass produced by the Westinghouse Savannah River Co (SRL 165 black frit). The shape of their sorption isotherms is qualitatively identical to those observed by Mazer et al. [7], and their desorption isotherms have a very similar shape, decreasing abruptly below $rH = 100\%$, then flattening to the lowest measured value at $rH = 3\%$, below which there must be a sharp additional decrease to $rH = 0\%$ that was not measured. Interestingly, however, their data show significant hysteresis (approximately twice the sorption observed in the sorption isotherm between $rH = 3\%$ and $rH = 60\%$) that does not close in the measured rH range. They also note that, even after desorption at $rH = 3\%$, several hours of exposure to high vacuum, sometimes with additional heating, were necessary to remove the rest of the water from the glass. Ebert et al. [8] attributed the hysteresis to condensation in pores, and the difficulty of final water removal to the presence of a strongly bonded surface monolayer. While the latter is reasonable, the former seems unlikely, as the shape of the desorption isotherm at high rH is unlike that expected for mesopores (it should initially be flat, then decrease sharply to the sorption value), and the hysteresis loop for a microporous solid should close well before $rH = 3\%$.

A more likely explanation for the hysteresis observed by Ebert et al. [8] is that it reflects reaction between the diffusing species and the glass matrix. As noted by Anovitz et al. [19], available evidence suggests that hydroxyl groups are present in powdered glasses hydrated at low temperatures, but this is probably mostly on the surface. Molecular water, however, has clearly diffused into obsidian. Even though there should be little reaction between it and the glass matrix, hysteresis is still expected in the sorption isotherms due to the time needed to remove the water from the glass.

The likely explanation for the differences between the published sorption isotherms [7,8] and our results is that the previous studies were performed on powdered samples, where ours report integrated diffusive sorption. The large surface areas of powders likely play an important role in the sorption process. Data such as ours, however, are clearly less dependent on surface effects and more reflective of properties of the bulk solid.

3.3. A model of diffusion with adsorption

If the experimental hydrogen concentration profiles are interpreted directly in terms of the water content of the glass, this suggests that the associated apparent diffusion coefficient is a function of concentration, and we have successfully employed this approach in previous studies [17,18,20]. An alternative model can, however, be obtained by considering diffusion in terms of the equilibrium pressure related to each concentration through the adsorption equilibrium. The consequence of adopting an adsorption model for the interaction between water and glass is that the adsorbate is assumed to exist as two phases in thermodynamic equilibrium: a condensed phase and a gas-like phase. The condensed phase, composed of the molecules remaining in direct contact with the surface, or with other adsorbed molecules, is much less mobile than the gas-like phase, so that all mass transfer can be assigned to the latter. In this model, the 'surface' refers to a conceptual, molecular-scale porosity within the glass framework in which the gas-like phase exists, not to the external surface of the sample. It is assumed that the same adsorption isotherm that governs the relation between the experimentally accessible relative humidity over the sample and the concentration at its external surface is also operative inside the glass framework. Regardless of the actual microstructural diffusion mechanism, the adsorption isotherm can be treated as a correlation between the concentration of the adsorbate on the solid surface and its pressure in the gas phase, which is a measure of its tendency to change phase and become mobile. The gradient of the equilibrium pressure, expressed as the relative pressure $p_r = p/p_0 = 0.01 \cdot rH$ then replaces the gradient of adsorbate concentration c as the driving force for diffusion.

For a constant diffusion coefficient, the changes with time t, and distance x, of the relative pressure of water p_r are described by Fick's second law, which is a second-order, linear partial differential equation,

$$\frac{\partial p_r(x,t)}{\partial t} = D \frac{\partial^2 p_r(x,t)}{\partial x^2}. \tag{6}$$

The solution to this equation for the semi-infinite problem with a constant boundary condition (the relative pressure at the surface equal to p_{r0i} for each of the experimental vessels) and a constant initial condition (the relative pressure uniformly equal to p_{r1} at the beginning of the experiment) leads to the set of functions:

$$p_{ri}(x,t) = (p_{r0i} - p_{r1})erfc\left(\frac{x}{2\sqrt{Dt}}\right) + p_{r1}, \tag{7}$$

for each data point (i) in the measured profile, which is the pressure analog of Eq. (2). It should be noted, however, that the assumption of a constant boundary condition contradicts the observation from our previous work [18,20]

that the surface concentration varies with time. Nonetheless, this simplifying assumption has been adopted for the purposes of this analysis as the relative humidity data were not collected as a function of time and available data (Anovitz et al., unpb.) at 100% rH suggests that most of the surface equilibration at this temperature is relatively rapid. The model presented here can, however, be modified to account for a time-dependent surface composition as well.

If the function $c_{ads}(p_r)$ describes the adsorption isotherm, then the equations for each data point:

$$c_{ads}[p_{ri}(x_{ij}, t)] = c_{ij}, \tag{8}$$

can be regressed simultaneously using the least squares method to fit the experimental concentration profile data pairs (x_{ij}, c_{ij}) and determine the adjustable parameters contained in $c_{ads}(p_r)$.

The initial choice for the adsorption equation was the BET Eq. (3) containing only three adjustable parameters. This approach, however, did not provide a good fit to the experimental concentration profiles at low pressures. Optimal fits, taking into account the uncertainty in the experimental data, were obtained using a rational function (Padé approximation) of the form

$$c_{ads}(a) = \frac{e_1 p_r + e_2 p_r^2 + e_3 p_r^3 + e_4 p_r^4}{1 + d_1 p_r + d_2 p_r^2 + d_3 p_r^3 + d_4 p_r^4}. \tag{9}$$

The relative pressure corresponding to the initial concentration c_1,

$$p_{r1} = c_{ads}^{-1}(c_1) \tag{10}$$

was treated as another adjustable parameter, in addition to the diffusion coefficient D, and the parameters e_i and d_i. The experimental profile data obtained very close to the sample surface, beyond the maximum concentration, were discarded. A number of synthetic data points were added at the deep end of the profiles at a concentration equal to the background value c_1 in order to extend the fit beyond the maximum depth where data were obtained and force the curve to equal the background value at depths beyond the hydrated layer.

The optimal values of the ten parameters are given in Table 3. In the selected fit the uncertainties of the parameters e_i and d_i were allowed to be arbitrarily large in order to provide the most flexibility and minimum systematic bias to Eq. (9). Since these parameters were only very weakly coupled to the physically meaningful parameters D and p_{r1}, the influence of the form of the Eq. (9) was minimized. For this reason, the uncertainties of the fit for the relevant parameters are quite small ($10^6 \cdot D = 1.539 \pm 0.02$ μm^2/s, $p_{r1} = 0.0051 \pm 0.002$). The overall accuracy of determination of D is estimated as better than 10%.

The resulting model profiles (continuous lines) are compared with experimental data in Fig. 8. Clearly, the model fits the data within the expected experimental uncertainty. The most notable deviations, observed in the profiles for nominal surface relative humidities $rH = 0.5$ and $rH =$

Table 3
Parameters of the model of diffusion with adsorption (Eqs. (7)–(9)) producing the best fit to the experimental concentration profiles

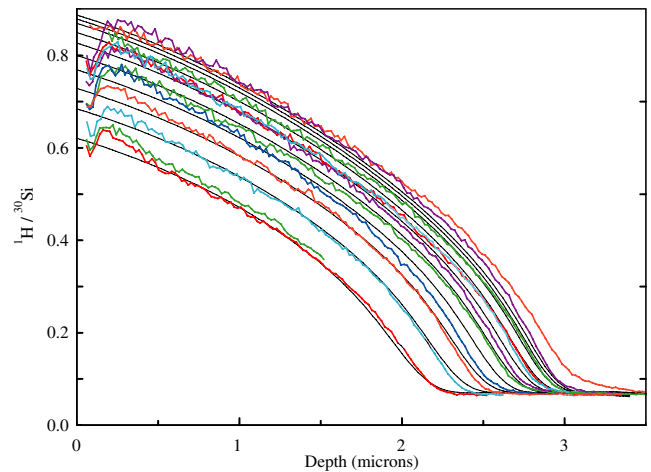| Parameter	Value
D	$1.53933 \cdot 10^{-6}$
a_1	0.00512510
e_1	12.0761463
e_2	−1117.06816
e_3	29098.8294
e_4	59905.6767
d_1	−50.87164975
d_2	172.343488
d_3	48807.0402
d_4	50111.9492

Fig. 8. Fit to the depth-profile data obtained using the diffusion with adsorption model.

1.0 that do not follow the general pattern, may have originated from analytical error.

The adsorption isotherm obtained from the model, Eq. (9), is compared in Fig. 3 with the BET isotherm, Eq. (3), which was obtained using solely the measured maximum concentrations and relative humidities on the surface. A good agreement was obtained in the region where surface concentration data are available (between $rH = 0.21$ and $rH = 1.0$). The shapes of the two adsorption isotherms are very similar, although Eq. (9), in contrast to the BET equation, does not carry any information about the physics of adsorption or a particular adsorption model. The inability of the BET isotherm to replace Eq. (9) in the region of the lowest water activities may be due to hydrophobic adsorption by very dry glass. As a result, the steep part of the adsorption isotherm is somewhat removed from the Y-axis, a feature the BET equation cannot accommodate. The isotherm in Fig. 3 could not be determined below the background concentration, $c_1 \approx 0.065$. Diffusion profile measurements on very well-dried samples (with a lower background concentration c_1), preferably also for lower surface humidities, would be necessary in order to determine the shape of the isotherm at very low humidity with greater precision.

Finally, it should be clarified why pressure (or relative pressure $p_r = p/p_0$), rather than fugacity, (or water activity $a = f/f_0$) was used as the driving force for diffusion. At 150 °C the differences between p_r and a are not significant in comparison with experimental error. The relative difference $100(a - p_r)/p_r$ increases from zero at the saturation pressure (4.757 bar) to a maximum of 4.2% at zero pressure. The least-squares fit was marginally better for relative pressures than for activities. This is also consistent with the common approach in which diffusion coefficients are written as a function of concentration, rather than activity. Nonetheless, it is clear from the above discussion that the adoption of the adsorption model, coupled with the assumption of gas-phase mass transfer, and following Fick's laws with a constant, concentration-independent diffusion coefficient, leads to a very satisfactory reproduction of the experimental concentration profiles.

4. Conclusions

The data presented in this paper clearly demonstrate that changes in relative humidity do affect the rate of glass hydration, at least under the conditions and for the glass composition tested. These effects are, however, relatively small at high rH values. In addition, we have shown that adsorption theory can be used successfully to model both the overall effects of relative humidity on surface concentration and diffusion rate, as well as the evolution of the diffusion profile.

From the point of view of obsidian hydration dating, the critical issue is the relative uncertainty imposed on an intrinsically calculated date by uncertainties in the relative humidity under which the sample was hydrated. The resultant uncertainty is, of course, a function of the total time involved. Fig. 9 shows the percentage of the actual time of the experiment that would be calculated for each profile assuming the diffusion coefficient calculated for the 100% relative humidity experiment. As can be seen, over the relative humidity range examined the calculated percentage effect is approximately linear, and the calculated age decreases by a factor of 2 at approximately 21% rH. Thus, over this range, and assuming a square-root-of-time dependence, a change in relative humidity of 1 percent will change the calculated age by approximately 0.62 percent.

The extent to which this effect is significant will depend on the particular site, its age, climatic variability and soil type, and the accuracy required for a given application. However, some general conclusions can be reached. Friedman et al. [9] measured the relative humidities of soils at 25 sites and depths between 0.01 and 2 m below the ground. The sites chosen represented a range from very dry to humid environments. They concluded that, at depths below 0.10 m in most environments, and about 0.25 m in hot-dry climates, the relative humidity was constant with depth and approximately equal to 100 percent.

This result is generally consistent with results from soil physics cf. [65]. With the exception of arctic and extreme
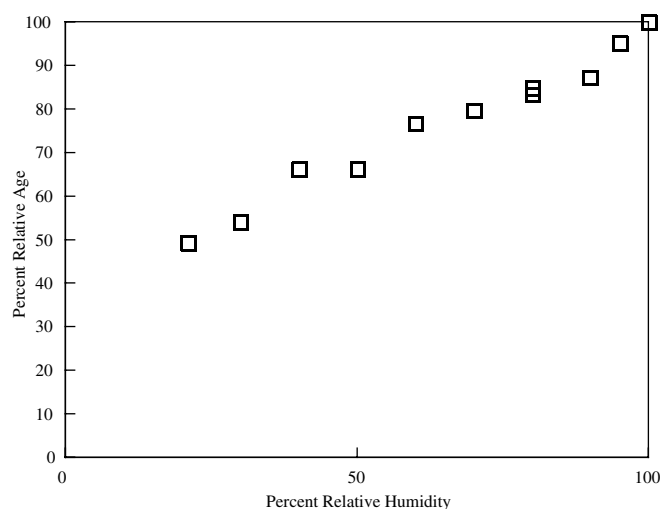

Fig. 9. The percentage of the actual time of the experiment that would be calculated for each profile assuming the diffusion coefficient calculated for the 100% relative humidity experiment. This provides an estimate of the changes in a calculated age of an artifact due to uncertainties in the relative humidity to which it was exposed.

desert conditions, most soils on earth are vegetated. Thus, the relative humidities of most soils must be high enough to support plant life. The water content of a soil below which water extraction by plants ceases, and the plants die is known as the permanent wilting percentage. While this is somewhat dependent on both plant and soil type, it is generally assumed to be equivalent to a water potential of −15 bars. Thus, to a first approximation, all vegetated soils have a water potential less than −15 bars, which is equivalent to a relative humidity of 98.9 percent at 25 °C. As noted by Hanks and Ashcroft [65], over this range the vapor pressure depression is too small to measure accurately using most standard techniques. Thus, these results are in good agreement with the data of Friedman et al. [9].

The implications of both our experimental data and the physical properties of most soils for obsidian hydration are reasonably clear. Under most common conditions variations of relative humidity are unlikely to have a significant effect on the rate of hydration of buried obsidians, especially once depths in excess of 0.1 to 0.25 m are reached.

These data also have interesting implications for hydration of glasses in other settings. For instance, if nuclear waste storage glasses behave in a manner similar to obsidian, very large reductions of relative humidity (below about 20% rH) will be needed before significant reductions in the rate of glass corrosion due to water diffusion, including the rate of perlite formation, are observed. This should be true even in a vapor-dominated atmosphere, where water-mediated corrosion due to leaching is expected to be minimal. Similar effects might be expected in a wide variety of industrial applications, although the extent to which these data, obtained on an alkali aluminosilicate glass, apply to glasses of vastly different compositions remains uncertain.

Acknowledgements

References

[1] I. Friedman, R. Smith, Am. Antiquity 25 (1960) 476.
[2] I. Friedman, R.L. Smith, W.D. Long, Geolog. Soc. Am Bulletin 77 (1966) 323.
[3] I. Friedman, I.W. Long, Science 191 (1976) 347.
[4] W.R. Ambrose, in: R.E. Taylor (Ed.), Advances in Obsidian Glass Studies, Noyes Press, New Jersey, 1976, p. 81.
[5] J.W. Michels, I.S.T. Tsong, G.A. Smith, Archaeometry 25 (1983) 107.
[6] J.W. Michels, I.S.T. Tsong, C.M. Nelson, Science 219 (1983) 361.
[7] J.J. Mazer, C.M. Stevenson, W.L. Ebert, J.K. Bates, Am. Antiquity 56 (1991) 504.
[8] W.L. Ebert, R.F. Hoburg, J.K. Bates, Phys. Chem. Glasses 32 (1991) 133.
[9] I. Friedman, F.W. Trembour, F.L. Smith, G.I. Smith, Quaternary Res. 41 (1994) 185.
[10] R.F. Bartholomew, B.L. Butler, H.L. Hoover, C.K. Wu, J. Am. Ceram. Soc. 63 (1980) 481.
[11] Y. Moriya, M. Nogami, J. Non-Cryst. Solids 38 & 39 (1980) 667.
[12] R.F. Bartholomew, J. Non-Cryst. Solids 56 (1983) 331.
[13] T. Yoko, Z.-J. Huang, K. Kamiya, S. Sakka, Intl. Congress Glass 13 (1983) 650.
[14] M. Tomozawa, S. Ito, J. Molinelli, J. Non-Cryst. Solids 64 (1984) 269.
[15] T.A. Abrajano, J.K. Bates, J.J. Mazer, J. Non-Cryst. Solids 108 (1989) 269.
[16] H. Tomozawa, M. Tomozawa, J. Non-Cryst. Solids 109 (1989) 311.
[17] L.M. Anovitz, J.M. Elam, L.R. Riciputi, D.R. Cole, J. Arch. Sci. 26 (1999) 735.
[18] L.M. Anovitz, J.M. Elam, L.R. Riciputi, D.R. Cole, Archaeometry 46 (2004) 301.
[19] L.M. Anovitz, L.R. Riciputi, D.R. Cole, M. Fayek, Amer. Mineral., submitted for publication.
[20] L.R. Riciputi, J.M. Elam, L.M. Anovitz, D.R. Cole, J. Arch. Sci. 29 (2002) 1055.
[21] P. Cohen, Water Coolant Technology of Power Reactors, 78, American Nuclear Society, New York, 1980.
[22] W.T. Lindsay Jr., in: P. Cohen (Ed.), The ASME Handbook on Water Technology for Thermal Power Systems, ASME, New York, 1989, p. 341.
[23] P.M. Wang, K.S. Pitzer, J.M. Simonson, J. Phys. Chem. Ref. Data 27 (1998) 971.
[24] M.S. Gruszkiewicz, J.M. Simonson, J. Chem. Thermodynamics 37 (2005) 906.
[25] K.S. Pitzer, J.C. Peiper, R.H. Busey, J. Phys. Chem. Ref. Data 13 (1984) 1.
[26] D.G. Archer, J. Phys. Chem. Ref. Data 21 (1992) 793.
[27] H.F. Gibbard Jr., G.J. Scatchard, Chem. Eng. Data 18 (1973) 293.
[28] H.F. Holmes, R.E. Mesmer, J. Phys. Chem. 87 (1983) 1242.
[29] M.S. Gruszkiewicz, unpublished.
[30] M.A. Styrikovich, I. Kh. Khaibullin, D.G. Tskhvirashvili, Doklady Akademii Nauk SSSR 100 (1955) 1123.
[31] R.R. Lee, D.A. Leich, T.A. Tombrello, J.E. Ericson, I. Friedman, Nature 250 (1974) 44.
[32] R.H. Doremus, J.Non-Cryst. Solids 19 (1975) 137.
[33] R.H. Doremus, in: M. Tomozawa, R.H. Doremus (Eds.), Treatise on Materials Science and Technology, vol. 17, Academic Press, New York, 1979, p. 41.
[34] R.H. Doremus, Glass Science, John Wiley and Sons, Inc., New York, 1994.
[35] W.A. Lanford, Science 196 (1977) 975.
[36] W.A. Lanford, Nucl. Instrum. Methods 149 (1978) 1.
[37] T. Laursen, W.A. Lanford, Nature 276 (1978) 53.
[38] I.S.T. Tsong, C.A. Houser, N.A. Yusef, R.F. Messier, W.B. White, J.W. Michels, Science 201 (1978) 339.
[39] I.S.T. Tsong, G.A. Smith, J.W. Michels, A.L. Wintenberg, P.D. Miller, C.D. Moak, Nucl. Instrum. Methods 191 (1981) 403.
[40] J. Garcia-Barcena, in: G.M. Gaxiola, J.E. Clark (Eds.), La Obsidiana en Mesoamerica. Mexico: Coleccion Cientifica, Serie Arqueologia, Instituto Nacional de Antropologia e Historia, 1989, p. 59-68.
[41] L. Haar, J.S. Gallagher, G.S. Kell, NBS/NRC Steam Tables, Hemisphere Publishing Corp., and McGraw- Hill, London, 1984.
[42] R.H. Doremus, Amer. Mineral. 85 (2000) 1674.
[43] L. Silver, E. Stolper, J. Petrol. 30 (1989) 667.
[44] L.M. Anovitz, J.M. Elam, L.R. Riciputi, D.R. Cole, M. Fayek, Geology 34 (2006) 517.
[45] J. Crank, Oxford University Press, Oxford, 1975.
[46] S. Brunauer, P.H. Emmett, E. Teller, J. Amer. Chem. Soc. 60 (1938) 309.
[47] S. Brunauer, The Adsorption of Gases and Vapors, Physical Adsorption, vol. 1, Princeton University Press, Princeton NJ, 1943.
[48] J.A. Barrie, in: J. Crank, G.S. Park (Eds.), Diffusion in Polymers, Academic Press, London, 1968, p. 259.
[49] S. Brunauer, J. Skalny, E.E. Bodor, J. Colloid Interf. Sci. 30 (1969) 546.
[50] S. Despond, E. Espuche, A. Domard, J. Polymer Sci. B, Polymer. Phys. 39 (2001) 3114.
[51] R.B. Anderson, J. Amer. Chem. Soc. 68 (1946) 686.
[52] J.H. De Boer, The Dynamical Character of Adsorption, second ed., Clarendon Press, Oxford, 1968.
[53] E.A. Guggenheim, Applications of Statistical Mechanics, Clarendon Press, Oxford, 1966.
[54] A.H. Harvey. National Institute of Standards and Technology, NISTIR 5068 (1998).
[55] T. Takei, A. Yamazaki, T. Watanabe, M. Chikazawa, J. Colloid Interf. Sci. 188 (1997) 409.
[56] J. Puibasset, R.J.-M. Pellenq, J. Chem. Phys. 118 (2003) 5613.
[57] J. Puibasset, R.J.-M. Pellenq, J Phys. Cond. Matter 16 (2004) S5329.
[58] H.W. Cremer, T. Davis, Chemical Engineering Practice, Butterworths, London, 1958, pp. 286.
[59] A. Sakoda, M. Suzuki, J. Chem. Eng., Jpn. 17 (1984) 52.
[60] K.C. Ng, H.T. Chua, C.Y. Chung, C.H. Loke, T. Kashiwagi, A. Akisawa, B.B. Saha, Appl. Thermal Eng. (2001) 1631.
[61] X. Wang, W. Zimmermann, K.C. Ng, A. Chakraboty, J.U. Keller, J. Thermal Anal. Calorim. 76 (2004) 659.
[62] A. Matsumoto, T. Sasaki, N. Nishimiya, K. Tsutsumi, Colloids Surf. A: Physicochem. Eng. Aspects 203 (2002) 185.
[63] M.S. Gruszkiewicz, J. Horita, J.M. Simonson, R.E. Mesmer, J.B. Hulen, Geothermics 30 (2001) 269.
[64] J. Hagymassy Jr., S. Brunauer, R.Sh. Mikhail, Colloid Interf. Sci. 29 (1969) 485.
[65] R.J. Hanks, G.L. Ashcroft, Applied Soil Physics, Springer-Verlag, Berlin, 1980.